Langmuir

ARTICLE

pubs.acs.org/Langmuir

Thermoresponsive Core Cross-Linked Micelles for Selective Ratiometric Fluorescent Detection of Hg^{2+} Ions

Xuejuan Wan, Tao Liu, and Shiyong Liu*

CAS Key Laboratory of Soft Matter Chemistry, Department of Polymer Science and Engineering, Hefei National Laboratory for Physical Sciences at the Microscale, University of Science and Technology of China, Hefei, Anhui 230026, China

Supporting Information

ABSTRACT: We report on the fabrication of core cross-linked (CCL) micelles possessing thermoresponsive cores and their application as sensitive and selective ratiometric Hg^{2+} probes with thermo-tunable detection efficiency. Well-defined double hydrophilic block copolymer (DHBC) bearing naphthalimide-based Hg^{2+}-reactive moieties (NUMA, **4**), PEO-*b*-P(NIPAM-*co*-NAS-*co*-NUMA), was synthesized via reversible addition−fragmentation chain transfer (RAFT) polymerization, where PEO, NIPAM, and NAS represent poly(ethylene oxide), *N*-isopropylacrylamide, and *N*-acryloxysuccinimide. At 25 °C, PEO-*b*-P(NIPAM-*co*-NAS-*co*-NUMA) unimers in aqueous solution can act as ratiometric Hg^{2+} probes with a detection limit of ∼10.1 nM. After core cross-linking of the micellar nanoparticles formed at elevated temperatures, structurally stable CCL micelles with well-solvated PEO coronas and thermoresponsive cores embedded with Hg^{2+}-reactive NUMA moieties were obtained. Upon Hg^{2+} addition, the aqueous dispersion of CCL micelles exhibit a colorimetric transition from yellowish to colorless and a fluorometric emission transition from green to bright blue. Moreover, Hg^{2+} detection limits of CCL micelles were considerably enhanced to 3.0 and 1.8 nM at 25 and 40 °C, when the thermoresponsive cores are at their swollen and collapsed state, respectively. The high selectivity of CCL micelles to Hg^{2+} over other common cations was also demonstrated. Furthermore, in vitro studies revealed that CCL micelles can effectively enter into living cells and sensitively respond to the presence of Hg^{2+} ions via the change of fluorescence emission color. This work represents the first example of DHBC-based CCL micelle acting as highly selective and sensitive ratiometric metal ion probes. The structural stability, water dispersibility, biocompatibility, and most importantly the thermo-tunable detection sensitivity of this novel type of CCL micelle-based sensing systems augur well for their future applications as multifunctional nanocarriers for drug delivery, sensing, imaging, and diagnosis.

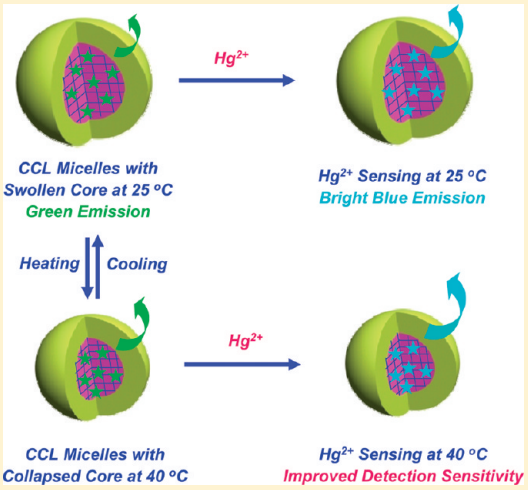

INTRODUCTION

The sensitive and selective detection of mercury pollutants both in vivo and in vitro is quite crucial considering their bioaccumulation, long residence, and permanent damage to central nervous and endocrine systems.[1,2] During the past decades, a variety of fluorometric and colorimetric mercury sensors have been fabricated from small organic molecules,[3−12] biomolecules,[13−19] conjugated polymers,[20−24] nanoparticles,[13,15,25−33] and polymeric assemblies.[34−37] Fluorometric Hg^{2+} probes are based on changes in either the relative fluorescence emission intensity or intensity ratio (if multiple emission bands are present) induced by the presence of Hg^{2+} ions. Compared to the former, the latter reports ratiometric values and can effectively eliminate the background interference and the fluctuation of detection conditions.[7,10,26,38−47]

Three main strategies have been employed to construct ratiometric fluorometric Hg^{2+} sensors. The first one relies on the utilization of fluorescence resonance energy transfer (FRET) principle.[10,38,43,46] Recently, Qian and his co-workers reported an elegant example of FRET-based small molecule ratiometric Hg^{2+} sensor by employing boron dipyrromethene dye (BODIPY) as the FRET donor and leuco-rhodamine derivative as the acceptor.[10] Taking advantage of the highly efficient ring-opening reaction of nonfluorescent rhodamine derivative induced by Hg^{2+}, ratiometric Hg^{2+} detection based on the "off−on" switching of FRET process can be achieved. The second strategy involves the utilization of an internal standard in combination with Hg^{2+}-responsive fluorescent moieties.[39,44] In a recent example, Zhang et al.[39] reported a ratiometric naphthalimide−porphyrin hybrid probe for Hg^{2+}, and the two Hg^{2+}-sensitive fluorophores possess almost independent fluorescent emission due to large differences (∼125 nm) in their maximum emission wavelengths and quite comparable excitation bands. This can effectively eliminate the FRET process between these two fluorophores. The third strategy for the design of ratiometric Hg^{2+} sensors is based on the intramolecular charge transfer (ICT) process by utilizing only

Received: December 10, 2010
Revised: February 11, 2011
Published: March 02, 2011

one type of fluorophore, the fluorescence emission band of which exhibits a remarkable shift upon binding with Hg^{2+} ions or reacting in the presence of Hg^{2+} ions.[7,26,41,45,48] In this context, Tian et al.[7] reported an Hg^{2+}-reactive ratiometric chemosensor based on naphthalimide phenylthiourea derivatives. Upon addition of Hg^{2+} ions, considerable ICT-induced shift of the fluorescence emission band occurs as the electron-donating amine moiety was replaced by less electron-rich guanidine functionality. Recently, we covalently attached a Hg^{2+}-sensing naphthalimide derivative into thermoresponsive poly(*N*-isopropylacrylamide) (PNIPAM) nanogels and fabricated polymeric nanoparticle-based ratiometric Hg^{2+} sensors with thermo-tunable detection sensitivity.[26]

Compared to small molecule fluorometric probes, sensing systems based on polymeric nanoparticles and assemblies can offer additional advantages such as improved water solubility, longer in vivo circulation times, and larger accumulation capacity due to the enhanced permeability and retention (EPR) effect; most importantly, the integration of multifunctions such as sensing, imaging, and therapeutics can also be achieved. In the past few years, our research work has mainly focused on the synthesis and self-assembly of stimuli-responsive amphiphilic and double hydrophilic block copolymers (DHBCs) with varying chain topologies.[49−53] To explore the applications of polymeric assemblies in sensing and detection, we recently reported the synthesis of well-defined DHBCs bearing rhodamine B derivatives (RhBHA) in the thermoresponsive block, poly(ethylene oxide)-*b*-P(NIPAM- *co*-RhBHA), PEO-*b*-P(NIPAM-*co*-RhBHA), which can serve as multifunctional sensors to pH, temperature, and Hg^{2+} ions.[35,54] Most importantly, the detection sensitivity to Hg^{2+} and pH could be dramatically enhanced at elevated temperature due to thermo-induced formation of micelles possessing hydrophobic cores. However, the detection protocol is mainly based on the changes in relative fluorescence emission intensity, and most importantly, micelles of PEO-*b*-P(NIPAM-*co*-RhBHA) are not stable at temperatures below the critical micellization temperature (CMT) and or at polymer concentrations below the critical micellization concentration (CMC). This will considerably limit their practical applications as polymeric assemblies-based sensing systems.[54]

In this context, several approaches such as core cross-linking (CCL) and shell cross-linking (SCL) have been proposed to enhance the structural stability of polymeric micelles.[55−60] Inspired by the work of McCormick et al.,[57] we previously reported the fabrication of reversible CCL micelles from PEO-*b*-P(NIPAM-*co*-NAS), which bears reactive acryloxysuccinimide (NAS) moieties.[61] Upon thermo-induced micellization, core cross-linking can be conveniently achieved by reaction of NAS residues in the micellar cores with a difunctional cross-linker, cystamine. In this work, we further attempted to utilize structurally stable CCL micelles with thermoresponsive cores as a platform to construct novel sensing systems (Scheme 1). We covalently attached Hg^{2+}-reactive moieties (NUMA) into the thermoresponsive block of PEO-*b*-P(NIPAM-*co*-NAS), and the obtained PEO-*b*- P(NIPAM-*co*-NAS-*co*-NUMA) DHBC can self-assemble into core−shell nanoparticles possessing thermoresponsive PNIPAM cores which can be cross-linked. We then determined and compared the Hg^{2+}-sensing capability of PEO-*b*-P(NIPAM-*co*-NAS-*co*-NUMA) unimers and CCL micelles at temperatures below and above the critical phase transition temperature. It was found that the aqueous dispersion of CCL micelles exhibits a colorimetric transition from yellowish to colorless and a fluorometric emission transition from green to bright blue upon addition of Hg^{2+} ions. Most importantly, the detection sensitivity to Hg^{2+} ions (~3.0 nM at 25 °C, ~1.8 nM at 40 °C) of CCL micelles constructed from PEO-*b*-P(NIPAM-*co*-NAS-*co*- NUMA) can be considerably enhanced compared to that at unimer state (~10.1 nM). The fluorescence imaging assay of Hg^{2+} ions in living cells was also investigated. As far as we know, this represents the first report of responsive DHBC-based CCL micelles which can act as highly selective and sensitive ratiometric probes for Hg^{2+} ions.

Scheme 1. Schematic Illustrations[a]

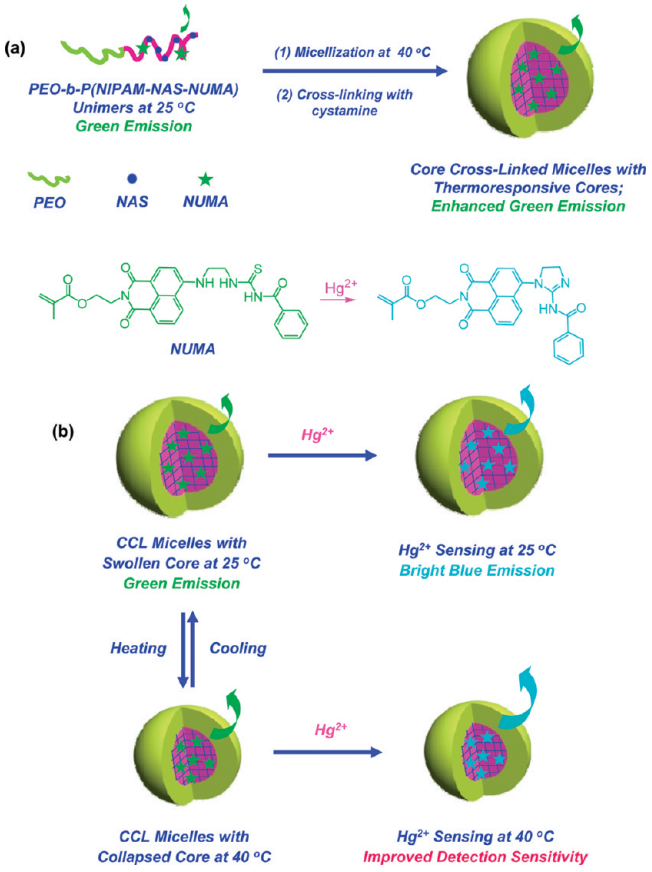

[a] (a) Preparation of core cross-linked (CCL) micelles with thermoresponsive cores from PEO-*b*-P(NIPAM-*co*-NAS-*co*-NUMA) diblock copolymer in aqueous solution and the Hg^{2+}-reactive mechanism of NUMA moieties. (b) Hg^{2+}-sensing capability of CCL micelles with improved detection sensitivity at elevated temperatures.

EXPERIMENTAL SECTION

Materials. *N*-Isopropylacrylamide (NIPAM, 97%, Tokyo Kasei Kagyo Co.) was purified by recrystallization from a mixture of benzene and *n*-hexane (1/3, v/v). Monohydroxy-capped poly(ethylene oxide), (PEO_{113}−OH, M_n = 5100, M_w/M_n = 1.10, mean degree of polymerization, DP, is 113) was purchased from Aldrich and used as received. 4-Bromo-1,8-naphthalic anhydride and methacrylic anhydride were purchased from Aldrich and used without further purification. Fetal bovine serum (FBS), penicillin, streptomycin, and Dulbecco's modified Eagle's medium (DMEM) were purchased from GIBCO and used as received. 2,2′-Azobisisobutyronitrile (AIBN, 98%, Fluka) was recrystallized from 95% ethanol. *N*-Hydroxysuccinimide (NHS, 97%, Aldrich) was recrystallized from toluene prior to use. *N*,*N*′-Dicyclohexylcarbodiimide (DCC), 4-dimethylaminopyridine (DMAP), potassium thiocyanate (KSCN), 2-aminoethanol, 1,2-ethylenediamine, benzoyl chloride,

Scheme 2. Schematic Illustration for the Synthesis of 1,8-Naphthalimide-Based Hg^{2+}-Reactive Polymerizable Monomer (NUMA, 4)

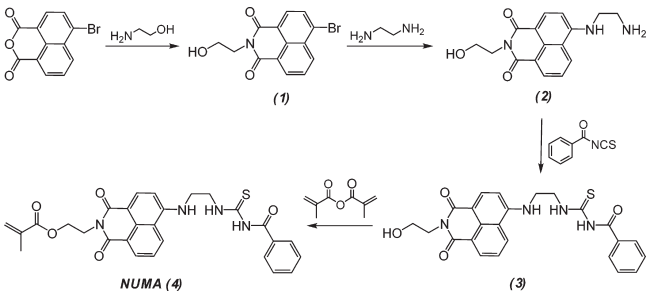

and all other reagents were purchased from Shanghai Chemical Reagent Co. and used as received. Benzoyl isothiocyanate,[62] *N*-acryloxysuccinimide (NAS),[63] and *S*-1-dodecyl-*S*′-(α,α′-dimethyl-α′′-acetic acid)trithiocarbonate (DDMATC)[64] were synthesized according to the literature procedures. Water was deionized with a Milli-Q SP reagent water system (Millipore) to a specific resistivity of 18.4 MΩ cm.

Sample Preparation. General approaches employed for the preparation of 1,8-naphthalimide based Hg^{2+}-sensing fluorescent monomer, NUMA (**4**), are shown in Scheme 2.

Preparation of 1,8-Naphthalimide-Based Hg^{2+}-Reactive Fluorescent Monomer (NUMA). The reaction of 4-bromo-1,8-naphthalic anhydride (2.77 g, 0.01 mol) and 2-aminoethanol (0.61 g, 0.01 mol) was conducted for 4 h in boiling 1,4-dioxane (50 mL) under magnetic stirring. After cooling to room temperature, the yellowish sediments were collected by filtration and then dried overnight at room temperature in a vacuum oven to give **1** (3.03 g, yield: 94.7%). ^{1}H NMR ($CDCl_3$, δ, ppm; Figure S1a): 8.64, 8.56, 8.40, 8.03, 7.85 (5H, naphthalimide-*H*), 4.45 (2H, $-CH_2CH_2OH$), 3.98 (2H, $-CH_2CH_2OH$).

A mixture of compound **1** (2.24 g, 7.0 mmol) and 1,2-ethylenediamine (12.6 g, 0.21 mol) in 80 mL 2-methoxylethanol was heated to reflux and stirred for 3 h. After cooling to room temperature, the reaction mixture was concentrated to 30 mL and poured into 200 mL water. Sediments were collected and then purified by recrystallization from chlorobenzene to give **2** as an orange solid (1.36 g, yield: 64.9%). ^{1}H NMR (DMSO-d_6, δ, ppm; Figure S1b): 8.64, 8.38, 8.18, 7.61, 6.74 (5H, naphthalimide-*H*), 4.06 (2H, $-CH_2CH_2OH$), 3.52 (2H, $-CH_2CH_2OH$), 2.81 (2H, $-NHCH_2CH_2NH_2$).

Compound **2** (0.90 g, 3 mmol) was dissolved in 30 mL dry acetone, and then freshly synthesized benzoyl isothiocyanate (0.49 g, 3 mmol) in 20 mL dry acetone was added dropwise over 1 h. The mixture was heated to 45 °C and allowed to stir for another 4 h. After cooling to room temperature, the sediments were collected by filtration and washed with dry acetone three times. The crude product was further purified by chromatography using ethyl acetate/CH_2Cl_2 as the eluent. After drying in a vacuum oven at room temperature overnight, **3** was obtained as an orange solid (0.87 g, yield: 62.7%). ^{1}H NMR (DMSO-d_6, δ, ppm; Figure S2a): 8.65, 8.48, 8.33, 7.95, 6.84 (5H, naphthalimide-*H*), 7.42−7.66 (5H, Ar-*H*), 4.26 (2H, $-CH_2CH_2OH$), 4.18 (2H, $-CH_2CH_2OH$), 3.74 (4H, $-NHCH_2CH_2NH-$).

A mixture of compound **3** (0.46 g, 1 mmol) and methacrylic anhydride (0.18 mL, 1.2 mmol) in 30 mL dry pyridine was stirred overnight at room temperature. The reaction mixture was then diluted with ethyl acetate and washed three times with saturated aqueous solution of $NaHCO_3$. The organic layer was collected and dried over anhydrous $MgSO_4$. After filtration, the filtrate was evaporated to dryness under reduced pressure. The crude product was further purified by chromatography using CH_2Cl_2 as eluent. After drying in a vacuum oven at room temperature overnight, NUMA (**4**) was obtained as an orange solid (0.37 g, 69.7% yield). ^{1}H NMR (DMSO-d_6, δ, ppm; Figure S2b): 8.64, 8.38, 8.21, 7.64, 6.93 (5H, naphthalimide-*H*), 7.83, 7.55, 7.44 (5H, Ar-*H*), 5.86, 5.13 (3H, $CH_2{=}CH(CH_3)-$), 4.71 (2H, $-CH_2CH_2OC{=}O$), 4.31 (2H, $-CH_2CH_2OC{=}O$), 4.06 (2H, $-NHCH_2CH_2NHC{=}S$), 3.97 (2H, $-NHCH_2CH_2NHC{=}S$), 2.13 (3H, $CH_2{=}CH(CH_3)-$).

Synthesis of PEO-b-P(NIPAM-co-NAS-co-NUMA) Diblock Copolymer. PEO macroRAFT agent was synthesized via the DCC-mediated esterification reaction of $PEO_{113}-OH$ with DDMATC according to literature procedures.[35] PEO-*b*-P(NIPAM-*co*-NAS-*co*-NUMA) diblock copolymer was prepared via RAFT copolymerization according to similar procedures we reported previously.[61] Typically, PEO_{113} macro-RAFT agent (0.54 g, 0.1 mmol), NIPAM (2.26 g, 20 mmol), NAS (0.38 g, 2.2 mmol), NUMA (57 mg, 0.11 mmol), and AIBN (3 mg, 0.02 mmol) were charged into a glass ampule containing 4 mL of 1,4-dioxane. The ampule was degassed through three freeze−thaw cycles, sealed under vacuum, and kept in an oil bath thermostatted at 70 °C to start the polymerization. After 2 h, the glass ampule was soaked into liquid nitrogen to quench the polymerization. The reaction mixture was diluted with THF and precipitated into an excess of diethyl ether. The sediments were collected and dried in a vacuum oven overnight at room temperature to obtain a yellowish green solid at a yield of 59%. The molecular weight and molecular weight distribution of PEO-*b*-P(NIPAM-*co*-NAS-*co*-NUMA) diblock copolymer were determined by GPC using THF as eluent, revealing an M_n of 18 200 and an M_w/M_n of 1.19 (Figure S3). The overall DP of P(NIPAM-*co*-NAS-*co*-NUMA) block and the NAS content were determined to be 110 and 16.0 mol %, respectively, by ^{1}H NMR analysis in $CDCl_3$ (Figure S4); thus, the copolymer was denoted as PEO_{113}-*b*-$P(NIPAM_{0.84}$-*co*-$NAS_{0.16}$-*co*-$NUMA)_{110}$. As the feed ratio of NUMA is quite low (∼0.5 mol %), its molar content (∼0.4 mol %) was determined by fluorescence measurements in methanol against a standard calibration curve.

Synthesis of CCL Micelles. 0.60 g PEO_{113}-*b*-$P(NIPAM_{0.84}$-*co*-$NAS_{0.16}$-*co*-$NUMA)_{110}$ was dissolved in 40 mL deionized water at 25 °C, and then heated to 40 °C. A bluish tinge characteristic of colloidal aggregates appeared upon heating, indicating the formation of micellar nanoparticles. After equilibration at 40 °C for 30 min, 8.1 mL aqueous solution of cystamine dihydrochloride (adjusted to pH 7, 5.0 g/L, 40 °C) was injected. The cystamine/NAS molar ratio was kept at 1:2. The reaction mixture was stirred for 5 h at 40 °C. After the mixture was cooled to 25 °C, the bluish tinge characteristic of micellar nanoparticles persisted, suggesting the successful core cross-linking.

Cell Culture and Fluorescence Imaging of Hg^{2+} Ions in Living Cells. HeLa cells were cultured in Dulbecco's modified Eagle medium (DMEM) supplemented with 10% FBS, penicillin (100 units/mL), and streptomycin (100 g/L) at 37 °C in a CO_2/air (5:95) incubator for 2 d. For fluorescence imaging, cells were first transferred to DMEM containing 1% FBS, and CCL micelles of PEO_{113}-*b*-$P(NIPAM_{0.84}$-*co*-$NAS_{0.16}$-*co*-$NUMA)_{110}$ (0.45 g/L, 10.0 μM NUMA residues) at 37 °C in a CO_2/air (5:95) incubator for 4 h; Hg^{2+} ions were then added to target a final concentration of 50.0 μM, and the mixture was further incubated for 30 min.

Characterization. All nuclear magnetic resonance (NMR) spectra were recorded on a Bruker 300 MHz spectrometer using $CDCl_3$ or DMSO-d_6 as the solvent. Molecular weights and molecular weight distributions were determined by gel permeation chromatography (GPC) equipped with a Waters 1515 pump and a Waters 2414 differential refractive index detector (set at 30 °C). It used a series of two linear Styragel columns (HR2 and HR4) at an oven temperature of 45 °C. The eluent was THF at a flow rate of 1.0 mL/min. A series of low-polydispersity polystyrene standards were employed for calibration. UV−vis spectra were acquired on a Unico UV/vis 2802PCS spectrophotometer. The transmittance of the aqueous solutions was acquired at a wavelength of 600 nm. A commercial spectrometer (ALV/DLS/SLS-5022F) equipped with a multitau digital time correlator (ALV5000) and

a cylindrical 22 mW Uniphase He−Ne laser (λ_0 = 632 nm) as the light source was employed for dynamic laser light scattering (LLS) measurements. Scattered light was collected at a fixed angle of 90° for duration of ~5 min. Distribution averages and particle size distributions were computed using cumulants analysis and CONTIN routines. All data were averaged over three measurements. Fluorescence spectra were recorded using a RF-5301/PC (Shimadzu) spectrofluorometer. The temperature of the water-jacketed cell holder was controlled by a programmable circulation bath. The slit widths were set at 5 nm for excitation and 5 nm for emission. The fluorescence images of HeLa cells incubated with CCL micelles in the presence and absence of Hg^{2+} ions were acquired on a Nikon Eclipse TE2000-U inverted microscopy.

RESULTS AND DISCUSSION

Well-defined DHBCs bearing Hg^{2+}-sensing moieties in the thermoresponsive block, PEO-*b*-P(NIPAM-*co*-NAS-*co*-NUMA), was synthesized via RAFT copolymerization by utilizing PEO-based macroRAFT agent.[65,66] The obtained diblock copolymer molecularly dissolves in aqueous solution at room temperature and self-assembles into core−shell nanoparticles consisting of thermoresponsive P(NIPAM-*co*-NAS-*co*-NUMA) cores and well-solvated PEO coronas. Upon core cross-linking at elevated temperatures, structurally stable CCL micelles was obtained, which can further serve as effective colorimetric and fluorometric probes to Hg^{2+} with thermo-tunable detection efficiency (Scheme 1).

Synthesis of 1,8-Naphthalimide-Based Hg^{2+}-Sensing Monomer (NUMA, 4), PEO-*b*-P(NIPAM-*co*-NAS-*co*-NUMA) DHBC, and Fabrication of CCL Micelles. The fluorescent monomer capable of fluorescent Hg^{2+}-sensing, NUMA (**4**), was synthesized in four steps as illustrated in Scheme 2. The reaction of 4-bromo-1,8-naphthalic anhydride with 2-aminoethanol afforded **1** at a relatively high yield. Its chemical structure was confirmed by ^{1}H NMR analysis, as evidenced by the appearance of resonance signals at 3.9 ppm (peak b) and 4.4 ppm (peak a) (Figure S1), which should be assigned to methylene protons adjacent to the amide functionality. Compound **2** was synthesized by the substitution reaction of **1** in the presence of 1,2-ethylenediamine. The ^{1}H NMR spectrum of **2** is also shown in Figure S1, together with the peak assignments. We can clearly observe the appearance of a new resonance signal at 2.9 ppm, which can be ascribed to methylene protons adjacent to the terminal primary amine group (peak i).

Compound **2** was then reacted with benzoyl isothiocyanate, and the subsequent esterification reaction of **3** with methacrylic anhydride finally afforded the target Hg^{2+}-sensing monomer **4**. ^{1}H NMR spectra of **3** and **4** are shown in Figure S2, together with the peak assignments. Compared to the NMR spectrum of **2**, new resonance signals characteristic of phenyl protons of **4** appeared in the range 7.4−7.6 ppm (peaks j, k, and l), accompanied by the presence of methacrylate double bond signals at 5.1 and 5.8 ppm. This indicates the successful preparation of Hg^{2+}-sensing monomer **4**.

Well-defined DHBCs bearing Hg^{2+}-sensing moieties in the thermoresponsive block, PEO-*b*-P(NIPAM-*co*-NAS-*co*-NUMA), was synthesized via RAFT copolymerization following similar protocols previously employed for the synthesis of PEO-*b*-P(NIPAM-*co*-NAS) diblock copolymer.[61] As expected, PEO-*b*-P(NIPAM-*co*-NAS-*co*-NUMA) molecularly dissolves in aqueous solution as unimers with an intensity-average hydrodynamic radius, $\langle R_h \rangle$, of 5−6 nm, and self-assembles at 40 °C into micelles with $\langle R_h \rangle$ of ~30 nm (Figure S5). The critical micellization temperature, CMT, was determined to be ~28 °C from the intercept of temperature-dependent optical transmittance curve (Figure 1). To enhance the structural stability of micelles of PEO-*b*-P(NIPAM-*co*-NAS-*co*-NUMA) formed at elevated temperatures, core cross-linking with cystamine was further conducted. After core cross-linking at 40 °C, dynamic LLS measurements revealed a $\langle R_h \rangle$ of ~37 nm for CCL micelles at 25 °C. This indicates the successful fabrication of CCL micelles possessing thermoresponsive cores; otherwise, micelles will dissociate into unimers at temperatures below the CMT (~28 °C).[61] We can also note from Figure S5 that, upon heating from 20 to 40 °C, $\langle R_h \rangle$ of CCL micelles decreases from 37 to 27 nm due to the thermo-induced collapse of cross-linked cores. Moreover, compared to that before cross-linking, the temperature-dependent optical transmittance of CCL micelles only exhibits slight changes with increasing temperatures (Figure 1).

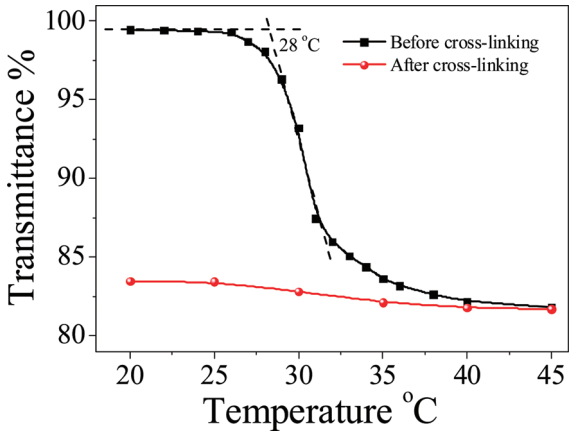

Figure 1. Temperature dependence of the optical transmittance at 800 nm obtained for 1.0 g/L aqueous solution of PEO_{113}-*b*-P-$(NIPAM_{0.84}$-*co*-$NAS_{0.16}$-*co*-NUMA$)_{110}$ diblock copolymer before and after core cross-linking.

CCL Micelles of PEO-*b*-P(NIPAM-*co*-NAS-*co*-NUMA) as Selective Colorimetric and Fluorometric Probes for Hg^{2+} Ions. Specially designed small molecules containing thiourea moieties have been frequently employed to construct Hg^{2+}-reactive colorimetric and fluorometric probes.[7,8,67−71] In 2007, Kim et al.[71] developed Hg^{2+} probes based on Hg^{2+}-triggered intramolecular guanylation of the reaction product from phenyl isothiocyanate and rhodamine 6G-ethylenediamine derivative. The guanylation reaction leads to the ring-opening of rhodamine 6G moiety initially in the spirolactam form, which is nonfluorescent. Thus, Hg^{2+}-triggered "off−on" switching of fluorescence emission can be achieved. However, the quantitative determination of Hg^{2+} can be only achieved through changes in relative fluorescence intensities. In another notable example, Tian et al.[7] synthesized small molecule probes from phenyl isothiocyanate and 1,8-naphthalimide-ethylenediamine derivative. In this case, Hg^{2+}-triggered guanylation reaction results in the replacement of electron-donating amine substituent on naphthalimide by the less electron-rich guanidine moiety. Thus, considerable change in the extent of ICT leads to a dramatic shift in the fluorescence emission band and, ratiometric quantification of Hg^{2+} ions can be achieved. However, this novel type of small molecule probe is subjected to poor water solubility, which partially limits their practical applications. In a previous report, we synthesized a Hg^{2+}-sensing polymerizable monomer by the reaction of acryloyl isothiocyanate with 1,8-naphthalimide-ethylenediamine derivative (NPTUA).[26] Thermoresponsive nanogels covalently

embedded with NPTUA were then synthesized and can act as selective Hg^{2+}-reactive colorimetric and fluorometric probes. Most importantly, we found that, at temperatures higher than the phase transition temperatures, the detection limit of Hg^{2+} ions can be considerably enhanced because collapsed nanogels provide a more hydrophobic microenvironment for the fluorescent dye and hence exhibit higher fluorescence quantum yield. In this work, we aim to establish that structurally stable CCL micelles can be employed as a platform to construct efficient Hg^{2+}-sensing systems (Scheme 1), so that multifunctional polymeric nanocarriers capable of sensing, imaging, and delivery of therapeutic agents can be fabricated.

For NUMA-labeled PEO-*b*-P(NIPAM-*co*-NAS-*co*-NUMA) diblock unimers in aqueous solution at room temperature, UV−vis absorption spectra upon gradual addition of Hg^{2+} ions were recorded (Figure S6). As the concentration of Hg^{2+} ions increased, the absorption band at 435 nm significantly decreased along with the growth of a new absorption band at ∼350 nm. This can be ascribed to Hg^{2+} ion-triggered intramolecular guanylation reaction (Scheme 1a). The aqueous solution also exhibits a colorimetric transition from yellowish to colorless due to the shift of absorption band into the UV region. From Figure S6, we can also observe the almost linear relationship between $A_0/(A - A_0)$ and $1/[Hg^{2+}]$ in the range 0−1.0 equiv Hg^{2+} ion relative to that of NUMA residues, where A_0 and A are absorbance intensities at 360 nm in the absence and presence of Hg^{2+} ions. This indicates that Hg^{2+} ion-triggered intramolecular guanylation reaction occurs in a stoichiometric manner. As an isoabsorptive point at 395 nm can be obtained from Figure S6, in subsequent sections, all fluorescence spectra were acquired at an excitation wavelength of 395 nm.

In the absence of Hg^{2+} ions, the aqueous solution of PEO-*b*-P(NIPAM-*co*-NAS-*co*-NUMA) exhibits intense green fluorescence emission centered at ∼532 nm, indicating that the copolymerization of NUMA into the thermoresponsive PNIPAM block does not affect the emission properties of NUMA (Figure 2). As the concentration of Hg^{2+} ions increased, the intramolecular guanylation reaction afforded naphthalimide derivatives exhibiting bright blue fluorescence emission at ∼485 nm. It has been well-established that the variation of electron-donating substituent at the 4-position of 1,8-naphthalimide can dramatically affect its fluorescence emission properties.[7,48,72] In the current case, the electron-rich secondary amine was replaced with a guanidine moiety which possesses much less electron-donating capability, and this led to a dramatic blue shift in the fluorescence emission.

The fluorometric titration spectra of PEO-*b*-P(NIPAM-*co*-NAS-*co*-NUMA) aqueous solution at 25 °C shown in Figure 2 indicated that, upon the addition of Hg^{2+} ions, the fluorescence intensity ratio (I_{485}/I_{532}) increased from 0.35 in the absence of Hg^{2+} to 1.92 in the presence of 1.5 equiv of Hg^{2+} ions, i.e., a ∼5.5-fold increase can be achieved. Note that the most prominent changes in emission intensity ratios occurred within the range 0−1.0 equiv Hg^{2+} ions, which agrees quite well with those shown in Figure S6. If the detection limit is defined as the Hg^{2+} concentration at which 10% change in fluorescence emission intensity ratio relative to the control can be observed, the detection limit of Hg^{2+} ions was determined to be 10.1 nM.

It is well-established that the quantum yield of certain fluorophores will be greatly enhanced when they are located in a more hydrophobic microenvironment.[73−75] As for PEO-*b*-P(NIPAM-*co*-NAS-*co*-NUMA) diblock copolymer, its thermo-induced micellization above the CMT will lead to the formation of micelles with hydrophobic domains embedded with NUMA dyes. The temperature-dependent fluorescence emission spectra of PEO-*b*-P(NIPAM-*co*-NAS-*co*-NUMA) aqueous solution in the absence of Hg^{2+} was then investigated (Figure 3). The fluorescence emission intensity exhibited a ∼3.1-fold enhancement in the temperature range 20−42 °C, accompanied with a slight blue shift from 532 to 523 nm.

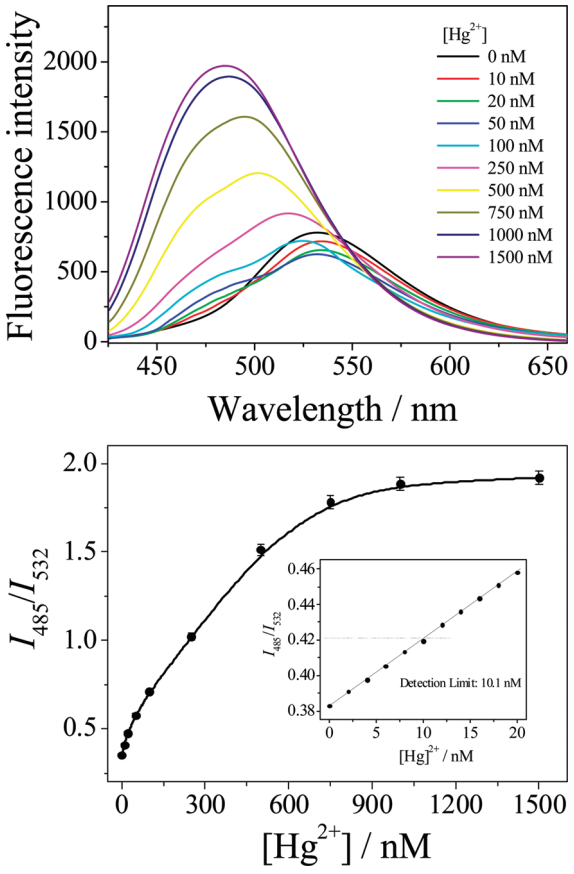

Figure 2. (a) Fluorescence emission spectra and (b) fluorescence intensity ratio changes (I_{485}/I_{532}) recorded for 0.045 g/L aqueous solution (1.0 μM NUMA residues) of PEO_{113}-*b*-P($NIPAM_{0.84}$-*co*-$NAS_{0.16}$-*co*-NUMA)$_{110}$ upon gradual addition of Hg^{2+} (0−1.5 equiv) at 25 °C. The spectra were recorded 20 min after Hg^{2+} addition (pH 7; λ_{ex} = 395 nm; slit widths: Ex = 5 nm, Em = 5 nm).

Taking advantage of the remarkable reactivity of NAS moieties toward primary amines,[57] the hydrophobic P(NIPAM-*co*-NAS-*co*-NUMA) core of micelles formed at elevated temperatures was cross-linked with cystamine to afford structurally stable CCL micelles. The fluorescence emission spectra of CCL micelles in aqueous solution at 40 °C upon addition of increasing amount of Hg^{2+} ions are shown in Figure 4. Note that the micellar cores are in their collapsed state at this temperature. A new fluorescence emission band can be clearly observed at ∼468 nm upon gradual addition of Hg^{2+} ions, and the intensity ratio, I_{468}/I_{523}, increased from 0.125 to 2.80 in the same range, i.e., ∼22-fold increase of emission intensity ratio can be achieved. Most importantly, the Hg^{2+} detection limit of CCL micelles at 40 °C was determined to be 1.8 nM, as compared to the detection limit of 10.1 nM for diblock unimers at 25 °C.

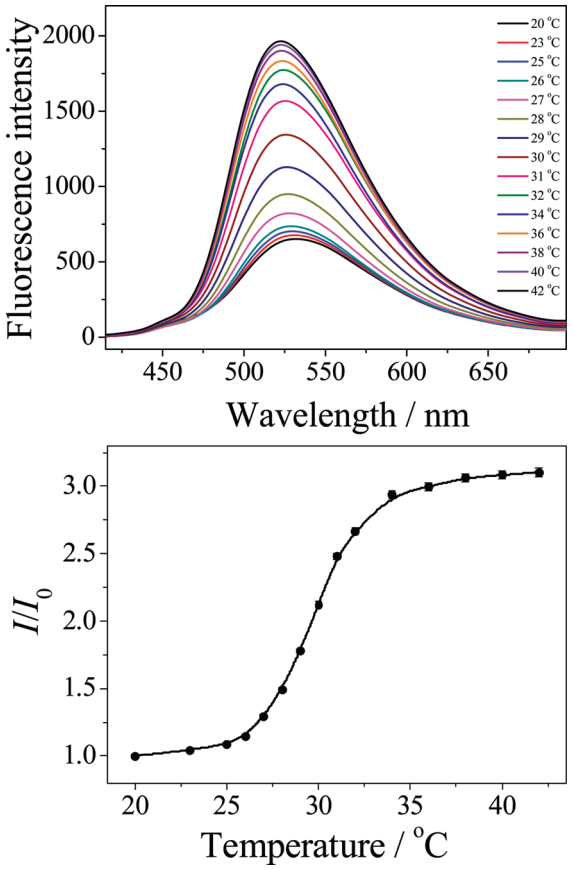

Figure 3. (a) Fluorescence emission spectra and (b) variation of relative fluorescence intensity recorded for 0.045 g/L aqueous solution (1.0 μM NUMA residues) of PEO_{113}-*b*-P(NIPAM$_{0.84}$-*co*-NAS$_{0.16}$-*co*-NUMA)$_{110}$ (pH 7; λ_{ex} = 395 nm; slit widths: Ex = 5 nm, Em = 5 nm) in the temperature range 20−42 °C.

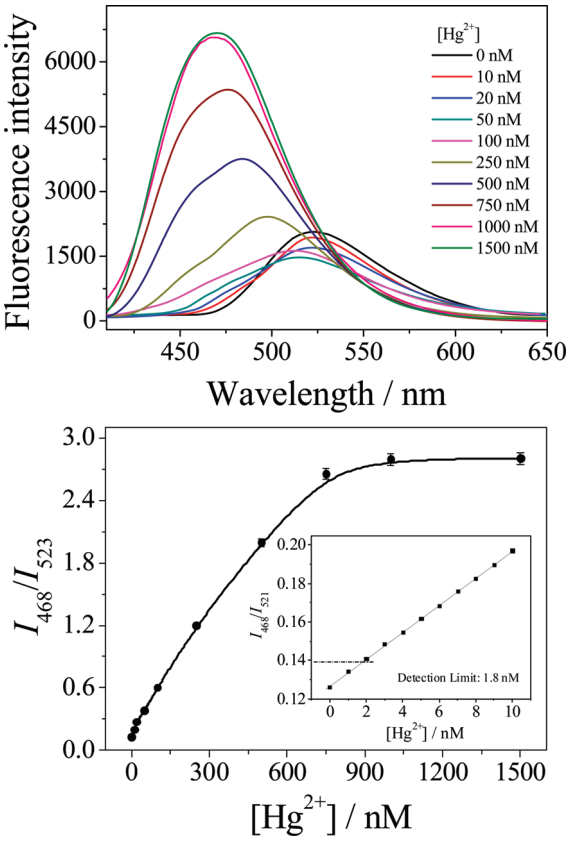

Figure 4. (a) Fluorescence emission spectra and (b) fluorescence intensity ratio changes (I_{468}/I_{523}) recorded for 0.045 g/L aqueous solution of CCL micelles (1.0 μM NUMA residues) upon gradual addition of Hg^{2+} (0−1.5 equiv) at 40 °C. The spectra were obtained 20 min after Hg^{2+} addition (pH 7; λ_{ex} = 395 nm; slit widths: Ex = 5 nm, Em = 5 nm).

For CCL micelles at 25 °C, NUMA moieties are located in a hydrophilic environment. In the Hg^{2+} concentration range 0−1.5 equiv relative to NUMA residues, the emission intensity ratio, I_{468}/I_{523}, increased from 0.165 to 2.4 (Figure 5). Note that, in the same Hg^{2+} concentration range, I_{468}/I_{523} increased ∼22-fold at 40 °C, which is larger than that at 25 °C (15-fold). Concomitantly, the detection limit of CCL micelles at 25 °C is ∼3.0 nM. The enhancement of detection limit for CCL micelles relative to that of diblock unimers at 25 °C, though in both cases, NUMA residues are in a hydrophilic microenvironment, that can be tentatively ascribed to the accumulation of NUMA dyes within the cores of CCL micelles. Thus, Hg^{2+} might have a higher probability to encounter and react with NUMA moieties, even at quite low concentrations. Moreover, the polarity of the cross-linked core might also be different from that of the P(NIPAM-*co*-NAS-*co*-NUMA) diblock unimer. In general, the above results successfully manifested that the structural integrity of CCL micelles can positively contribute to the detection performance. The changes of relative fluorescence intensities, I/I_0, of the emission band associated with the Hg^{2+}-triggered product can also be employed for the quantitative determination of Hg^{2+} ions. Figure 6 shows the Hg^{2+} concentration-dependent emission intensities of diblock unimers at 25 °C (485 nm) and CCL micelles at 25 and 45 °C (468 nm). In all three cases, the Hg^{2+} detection limits were determined to be 16.7 nM, 4.8 nM, and 3.8 nM, respectively.

The detection selectivity of CCL micelles fabricated from PEO-*b*-P(NIPAM-*co*-NAS-*co*-NUMA) toward Hg^{2+} ions over other common cations such as Na^+, K^+, Pb^{2+}, Cu^{2+}, Ag^+, Zn^{2+}, Fe^{2+}, Fe^{3+}, and Hg^{2+} was also investigated (Figures 7 and 8). Among all the cations used in the measurements, only Hg^{2+} exhibits apparent colorimetric and fluorometric changes. The presence of Hg^{2+} ions lead to a colorimetric transition from yellowish to colorless and a fluorometric transition from green to bright, which can even be discerned by the naked eye (Figure 8). It is worth noting that, at extended time periods, Ag^+ can also trigger the intramolecular guanylation reaction of NUMA residues, but it takes a much longer time (∼20 h) to complete. Moreover, the existence of Cu^{2+} ions exhibits no interference for the measurement, demonstrating that the CCL micelle-based detection system possesses promising advantages in discriminating among Ag^+, Hg^{2+}, and Cu^{2+} ions.

Finally, we investigated the Hg^{2+} sensing capacity of CCL micelles in living cells. As shown in Figure 9a, HeLa cells cultured in the presence of 0.45 g/L CCL micelles exhibit green fluorescence, indicating that CCL micelles can effectively enter into cells. When the above culture mixture was supplemented with 5.0 equiv Hg^{2+} (relative to NUMA residues) for 30 min, a distinctive fluorometric transition from green to blue can be clearly observed by fluorescence microscopy (Figure 9b). This preliminary experiment indicates that

dx.doi.org/10.1021/la104911r |*Langmuir* 2011, 27, 4082–4090

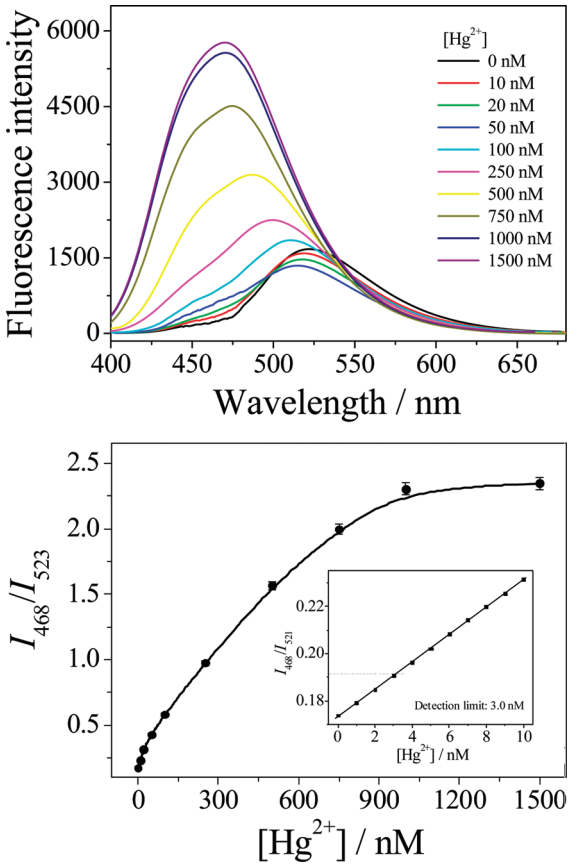

Figure 5. (a) Fluorescence emission spectra and (b) fluorescence intensity ratio changes (I_{468}/I_{523}) recorded for 0.045 g/L aqueous solution of CCL micelles (1.0 μM NUMA residues) upon gradual addition of Hg^{2+} (0−1.5 equiv) at 25 °C. The spectra were obtained 20 min after Hg^{2+} addition (pH 7; λ_{ex} = 395 nm; slit widths: Ex = 5 nm, Em = 5 nm).

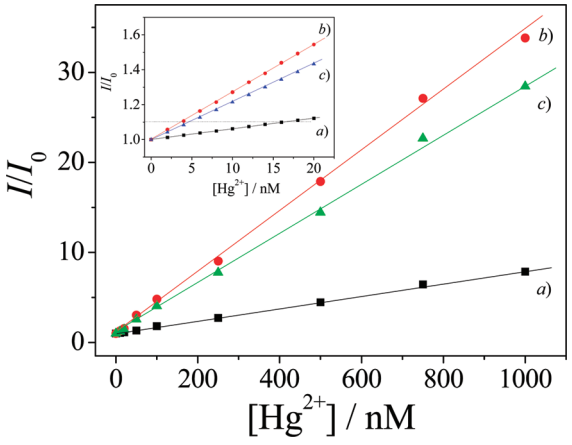

Figure 6. Variation of relative fluorescence intensity recorded for 0.045 g/L aqueous dispersion (1.0 μM NUMA residues) of (a) PEO_{113}-*b*-P-$(NIPAM_{0.84}$-*co*-$NAS_{0.16}$-*co*-$NUMA)_{110}$ at 25 °C (λ_{em} = 485 nm), (b) CCL micelles at 40 °C (λ_{em} = 468 nm), and (c) CCL micelles at 25 °C (λ_{em} = 468 nm) upon gradual addition of Hg^{2+} (0−1.5 equiv), respectively (λ_{ex} = 395 nm; slit widths: Ex = 5 nm, Em = 5 nm).

CCL micelles bearing Hg^{2+}-reactive NUMA moieties can be employed for cell imaging of Hg^{2+} ions. Moreover, the bright field image shown in Figure 9c revealed that cells are generally

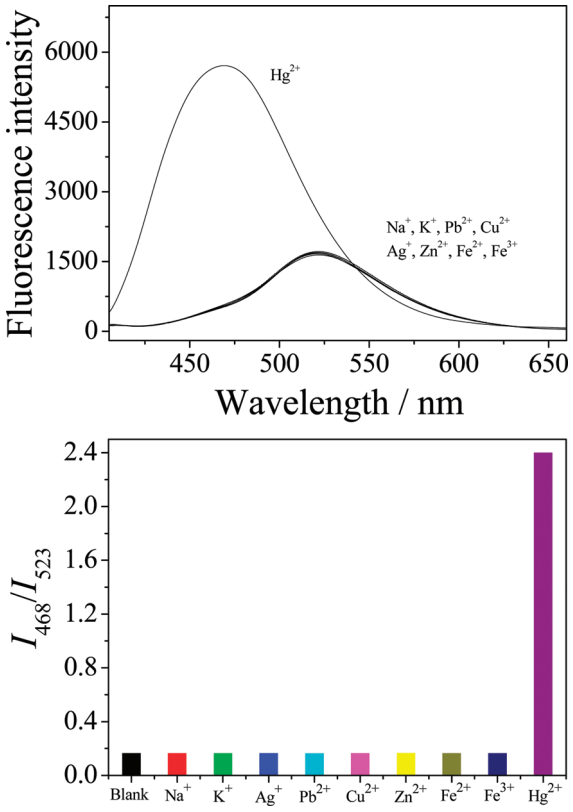

Figure 7. (a) Fluorescence emission spectra and (b) fluorescence intensity ratio changes of 0.045 g/L CCL micelles (1.0 μM NUMA residues) (pH 7, 25 °C) in the presence of 5.0 equiv of Na^+, K^+, Ag^+, Co^{2+}, Pb^{2+}, Cu^{2+}, Zn^{2+}, Cd^{2+}, Fe^{2+}, Fe^{3+}, and Hg^{2+}, respectively. The spectra were obtained 20 min after addition of various ions (λ_{ex} = 390 nm, slit widths: Ex = 5 nm, Em = 5 nm).

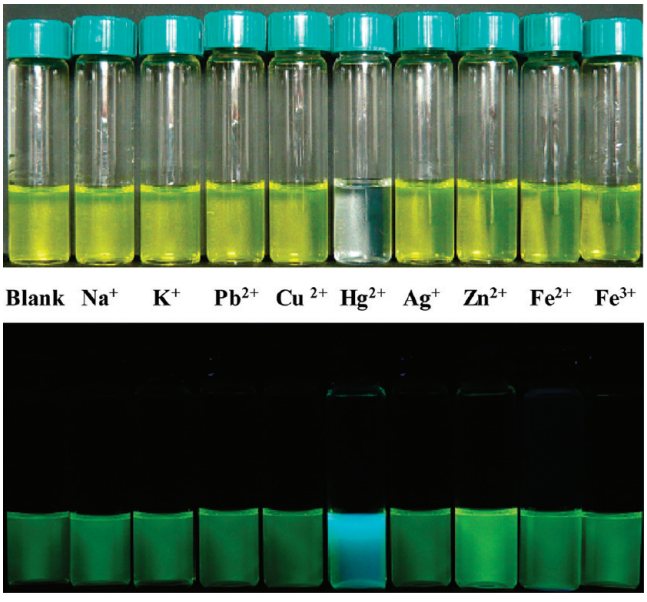

Figure 8. Optical photographs recorded under visible light (top) and UV (365 nm, bottom) for 2.0 g/L CCL micelles 1 h after the addition of 5.0 equiv of Na^+, K^+, Pb^{2+}, Cu^{2+}, Hg^{2+}, Ag^+, Zn^{2+}, Fe^{2+}, and Fe^{3+}, respectively.

viable throughout the culture process. The above results augur well for the further development of multifunctional CCL

dx.doi.org/10.1021/la104911r |*Langmuir* 2011, 27, 4082–4090

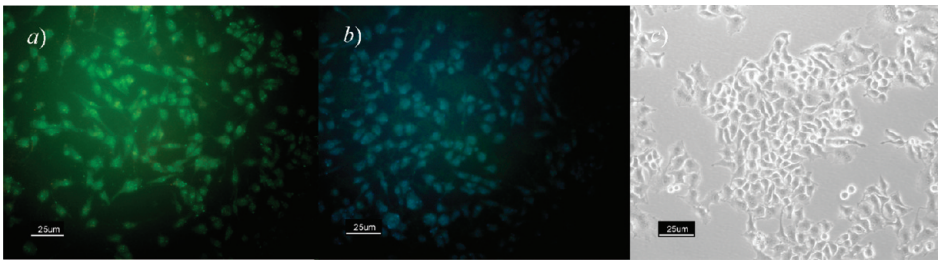

Figure 9. Fluorescent images (340/380 nm excitation filter in combination with long pass 420 nm barrier filter) of (a) HeLa cells incubated with 0.45 g/L CCL micelles (10.0 μM NUMA residues) at 37 °C for 4 h, (b) HeLa cells incubated with 0.45 g/L CCL micelles (10.0 μM NUMA residues) at 37 °C for 4 h and then with 50.0 μM Hg^{2+} for 30 min, and (c) a bright field image of the cells in panel (b).

micelles capable of sensing, imaging, and controlled delivery and release of therapeutic agents.

CONCLUSION

In summary, we reported on the preparation of CCL micelles and their application as sensitive and selective ratiometric Hg^{2+} sensors with thermo-tunable detection efficiency. Well-defined DHBCs bearing naphthalimide-based Hg^{2+}-reactive moieties, NUMA, in the thermoresponsive block, PEO-*b*-P(NIPAM-*co*-NAS-*co*-NUMA), were synthesized via RAFT polymerization. The obtained DHBCs served as a ratiometric chemosensor for Hg^{2+} with a detection limit of ~10.1 nM in their unimer state. Upon core cross-linking at elevated temperatures, the structurally stable CCL micelles with well-solvated PEO coronas and NUMA-labeled thermoresponsive cores exhibited a considerable enhancement in detection limit for Hg^{2+}, i.e., 3.0 nM and 1.8 nM at 25 and 40 °C, as the thermoresponsive cores are at their swollen and collapsed state, respectively. In vivo fluorescence imaging assay of Hg^{2+} ion suggested that the obtained CCL micelle sensors can effectively enter into living cells and sensitively respond to Hg^{2+} ions. It should be noted that this work represents the first example of responsive DHBC-based CCL micelle as chemosensors for the sensitive ratiometric detection of Hg^{2+} ions with excellent selectivity. The reported CCL micelle-based sensing system possesses combined advantages such as structural stability, water dispersibility, and biocompatibility, and most importantly, the thermo-tunable detection sensitivity endowed them with potential applications in multifunctional nanocarriers.

ASSOCIATED CONTENT

Supporting Information. Additional figures as described in the text. This material is available free of charge via the Internet at http://pubs.acs.org.

AUTHOR INFORMATION

Corresponding Author

*To whom correspondence should be addressed. E-mail: sliu@ustc.edu.cn.

ACKNOWLEDGMENT

The financial support from National Natural Scientific Foundation of China (NNSFC) Projects (20874092, 91027026, and 51033005), Fundamental Research Funds for the Central Universities, and Specialized Research Fund for the Doctoral Program of Higher Education (SRFDP) is gratefully acknowledged.

REFERENCES

(1) Boening, D. W. *Chemosphere* **2000**, *40*, 1335–1351.
(2) Clarkson, T. W.; Magos, L.; Myers, G. J. *N. Engl. J. Med.* **2003**, *349*, 1731–1737.
(3) Kim, H. N.; Lee, M. H.; Kim, H. J.; Kim, J. S.; Yoon, J. *Chem. Soc. Rev.* **2008**, *37*, 1465–1472.
(4) Nolan, E. M.; Lippard, S. J. *Chem. Rev.* **2008**, *108*, 3443–3480.
(5) Yoon, S.; Miller, E. W.; He, Q.; Do, P. H.; Chang, C. J. *Angew. Chem., Int. Ed.* **2007**, *46*, 6658–6661.
(6) Wang, J. B.; Qian, X. H. *Chem. Commun.* **2006**, 109–111.
(7) Liu, B.; Tian, H. *Chem. Commun.* **2005**, 3156–3158.
(8) Yang, Y. K.; Yook, K. J.; Tae, J. *J. Am. Chem. Soc.* **2005**, *127*, 16760–16761.
(9) Lee, M. H.; Wu, J. S.; Lee, J. W.; Jung, J. H.; Kim, J. S. *Org. Lett.* **2007**, *9*, 2501–2504.
(10) Zhang, X. L.; Xiao, Y.; Qian, X. H. *Angew. Chem., Int. Ed.* **2008**, *47*, 8025–8029.
(11) Caballero, A.; Martinez, R.; Lloveras, V.; Ratera, I.; Vidal-Gancedo, J.; Wurst, K.; Tarraga, A.; Molina, P.; Veciana, J. *J. Am. Chem. Soc.* **2005**, *127*, 15666–15667.
(12) Shi, W.; Sun, S. N.; Li, X. H.; Ma, H. M. *Inorg. Chem.* **2010**, *49*, 1206–1210.
(13) Freeman, R.; Finder, T.; Willner, I. *Angew. Chem., Int. Ed.* **2009**, *48*, 7818–7821.
(14) Liu, C. W.; Huang, C. C.; Chang, H. T. *Anal. Chem.* **2009**, *81*, 2383–2387.
(15) Guo, W. W.; Yuan, J. P.; Wang, E. K. *Chem. Commun.* **2009**, 3395–3397.
(16) Chen, P.; He, C. A. *J. Am. Chem. Soc.* **2004**, *126*, 728–729.
(17) Ono, A.; Togashi, H. *Angew. Chem., Int. Ed.* **2004**, *43*, 4300–4302.
(18) Dave, N.; Chan, M. Y.; Huang, P. J. J.; Smith, B. D.; Liu, J. W. *J. Am. Chem. Soc.* **2010**, *132*, 12668–12673.
(19) Chan, D. S. H.; Lee, H. M.; Che, C. M.; Leung, C. H.; Ma, D. L. *Chem. Commun.* **2009**, 7479–7481.
(20) Thomas, S. W.; Joly, G. D.; Swager, T. M. *Chem. Rev.* **2007**, *107*, 1339–1386.
(21) Liu, X. F.; Tang, Y. L.; Wang, L. H.; Zhang, J.; Song, S. P.; Fan, C. H.; Wang, S. *Adv. Mater.* **2007**, *19*, 1471–1474.
(22) Liu, S. J.; Fang, C.; Zhao, Q.; Fan, Q. L.; Huang, W. *Macromol. Rapid Commun.* **2008**, *29*, 1212–1215.
(23) Kim, I. B.; Bunz, U. H. F. *J. Am. Chem. Soc.* **2006**, *128*, 2818–2819.
(24) Qin, C. J.; Wu, X. F.; Gao, B. X.; Tong, H.; Wang, L. X. *Macromolecules* **2009**, *42*, 5427–5429.
(25) Lee, J. S.; Han, M. S.; Mirkin, C. A. *Angew. Chem., Int. Ed.* **2007**, *46*, 4093–4096.
(26) Li, C. H.; Liu, S. Y. *J. Mater. Chem.* **2010**, *20*, 10716–10723.
(27) Lee, J. S.; Mirkin, C. A. *Anal. Chem.* **2008**, *80*, 6805–6808.

(28) Huang, C. C.; Yang, Z.; Lee, K. H.; Chang, H. T. *Angew. Chem., Int. Ed.* **2007**, *46*, 6824–6828.
(29) Rex, M.; Hernandez, F. E.; Campiglia, A. D. *Anal. Chem.* **2006**, *78*, 445–451.
(30) Darbha, G. K.; Ray, A.; Ray, P. C. *ACS Nano* **2007**, *1*, 208–214.
(31) Lee, S. J.; Lee, J. E.; Seo, J.; Jeong, I. Y.; Lee, S. S.; Jung, J. H. *Adv. Funct. Mater.* **2007**, *17*, 3441–3446.
(32) Adhikari, B.; Banerjee, A. *Chem. Mater.* **2010**, *22*, 4364–4371.
(33) Bera, R. K.; Das, A. K.; Raj, C. R. *Chem. Mater.* **2010**, *22*, 4505–4511.
(34) Sasaki, D. Y.; Padilla, B. E. *Chem. Commun.* **1998**, 1581–1582.
(35) Hu, J. M.; Li, C. H.; Liu, S. Y. *Langmuir* **2010**, *26*, 724–729.
(36) Zhao, Y.; Zhong, Z. Q. *Org. Lett.* **2006**, *8*, 4715–4717.
(37) Zhang, X. B.; Guo, C. C.; Li, Z. Z.; Shen, G. L.; Yu, R. Q. *Anal. Chem.* **2002**, *74*, 821–825.
(38) Ben Othman, A.; Lee, J. W.; Wu, J. S.; Kim, J. S.; Abidi, R.; Thuery, P.; Strub, J. M.; Van Dorsselaer, A.; Vicens, J. *J. Org. Chem.* **2007**, *72*, 7634–7640.
(39) Li, C. Y.; Zhang, X. B.; Qiao, L.; Zhao, Y.; He, C. M.; Huan, S. Y.; Lu, L. M.; Jian, L. X.; Shen, G. L.; Yu, R. Q. *Anal. Chem.* **2009**, *81*, 9993–10001.
(40) Nolan, E. M.; Lippard, S. J. *J. Mater. Chem.* **2005**, *15*, 2778–2783.
(41) Yuan, M. J.; Li, Y. L.; Li, J. B.; Li, C. H.; Liu, X. F.; Lv, J.; Xu, J. L.; Liu, H. B.; Wang, S.; Zhu, D. *Org. Lett.* **2007**, *9*, 2313–2316.
(42) Nolan, E. M.; Lippard, S. J. *J. Am. Chem. Soc.* **2007**, *129*, 5910–5918.
(43) Coskun, A.; Akkaya, E. U. *J. Am. Chem. Soc.* **2006**, *128*, 14474–14475.
(44) Wegner, S. V.; Okesli, A.; Chen, P.; He, C. A. *J. Am. Chem. Soc.* **2007**, *129*, 3474–3475.
(45) Nguyen, D. M.; Frazer, A.; Rodriguez, L.; Belfield, K. D. *Chem. Mater.* **2010**, *22*, 3472–3481.
(46) Xu, M. Y.; Wu, S. Z.; Zeng, F.; Yu, C. M. *Langmuir* **2010**, *26*, 4529–4534.
(47) Guo, Z. Q.; Zhu, M. M.; Wu, X. M.; Tian, H. *Chem.—Eur. J.* **2010**, *16*, 14424–14432.
(48) Leng, B.; Zou, L.; Jiang, J. B.; Tian, H. *Sens. Actuator, B* **2009**, *140*, 162–169.
(49) Ge, Z. S.; Zhou, Y. M.; Xu, J.; Liu, H. W.; Chen, D. Y.; Liu, S. Y. *J. Am. Chem. Soc.* **2009**, *131*, 1628–1629.
(50) Ge, Z. S.; Xu, J.; Hu, J. M.; Zhang, Y. F.; Liu, S. Y. *Soft Matter* **2009**, *5*, 3932–3939.
(51) Li, C. H.; Ge, Z. S.; Fang, J.; Liu, S. Y. *Macromolecules* **2009**, *42*, 2916–2924.
(52) Rao, J. Y.; Luo, Z. F.; Ge, Z. S.; Liu, H.; Liu, S. Y. *Biomacromolecules* **2007**, *8*, 3871–3878.
(53) Butun, V.; Liu, S.; Weaver, J. V. M.; Bories-Azeau, X.; Cai, Y.; Armes, S. P. *React. Funct. Polym.* **2006**, *66*, 157–165.
(54) Hu, J. M.; Liu, S. Y. *Macromolecules* **2010**, *43*, 8315–8330.
(55) Thurmond, K. B.; Kowalewski, T.; Wooley, K. L. *J. Am. Chem. Soc.* **1996**, *118*, 7239–7240.
(56) Guo, A.; Liu, G. J.; Tao, J. *Macromolecules* **1996**, *29*, 2487–2493.
(57) Li, Y. T.; Lokitz, B. S.; McCormick, C. L. *Macromolecules* **2006**, *39*, 81–89.
(58) Jiang, X. Z.; Liu, S. Y.; Narain, R. *Langmuir* **2009**, *25*, 13344–13350.
(59) Jiang, X. Z.; Luo, S. Z.; Armes, S. P.; Shi, W. F.; Liu, S. Y. *Macromolecules* **2006**, *39*, 5987–5994.
(60) Jiang, X. Z.; Zhang, G. Y.; Narain, R.; Liu, S. Y. *Soft Matter* **2009**, *5*, 1530–1538.
(61) Zhang, J. Y.; Jiang, X.; Zhang, Y. F.; Li, Y. T.; Liu, S. Y. *Macromolecules* **2007**, *40*, 9125–9132.
(62) Wei, T. B.; Lin, Q.; Zhang, Y. M.; Wei, W. *Synth. Commun.* **2004**, *34*, 181–186.
(63) Pollak, A.; Blumenfeld, H.; Wax, M.; Baughn, R. L.; Whitesides, G. M. *J. Am. Chem. Soc.* **1980**, *102*, 6324–6336.
(64) Lai, J. T.; Filla, D.; Shea, R. *Macromolecules* **2002**, *35*, 6754–6756.
(65) Scales, C. W.; Convertine, A. J.; McCormick, C. L. *Biomacromolecules* **2006**, *7*, 1389–1392.
(66) Nuopponen, M.; Ojala, J.; Tenhu, H. *Polymer* **2004**, *45*, 3643–3650.
(67) Hennrich, G.; Sonnenschein, H.; Resch-Genger, U. *J. Am. Chem. Soc.* **1999**, *121*, 5073–5074.
(68) Ko, S. K.; Yang, Y. K.; Tae, J.; Shin, I. *J. Am. Chem. Soc.* **2006**, *128*, 14150–14155.
(69) Yang, Y. K.; Ko, S. K.; Shin, I.; Tae, J. *Nat. Protoc.* **2007**, *2*, 1740–1745.
(70) Lee, M. H.; Cho, B. K.; Yoon, J.; Kim, J. S. *Org. Lett.* **2007**, *9*, 4515–4518.
(71) Wu, J. S.; Hwang, I. C.; Kim, K. S.; Kim, J. S. *Org. Lett.* **2007**, *9*, 907–910.
(72) Srikun, D.; Miller, E. W.; Dornaille, D. W.; Chang, C. J. *J. Am. Chem. Soc.* **2008**, *130*, 4596–4597.
(73) Uchiyama, S.; Kawai, N.; de Silva, A. P.; Iwai, K. *J. Am. Chem. Soc.* **2004**, *126*, 3032–3033.
(74) Zhu, M. Q.; Zhu, L. Y.; Han, J. J.; Wu, W. W.; Hurst, J. K.; Li, A. D. Q. *J. Am. Chem. Soc.* **2006**, *128*, 4303–4309.
(75) Uchiyama, S.; Matsumura, Y.; de Silva, A. P.; Iwai, K. *Anal. Chem.* **2003**, *75*, 5926–5935.